Matrix Biology 35 (2014) 91–102

Contents lists available at ScienceDirect

Matrix Biology

journal homepage: www.elsevier.com/locate/matbio

A decorin-deficient matrix affects skin chondroitin/dermatan sulfate levels and keratinocyte function☆

Katerina Nikolovska [a,1], Jana K. Renke [a,1], Oliver Jungmann [a], Kay Grobe [a], Renato V. Iozzo [b], Alina D. Zamfir [c], Daniela G. Seidler [a,*]

[a] Insitute of Physiological Chemistry and Pathobiochemistry, Waldeyerstr. 15, University Hospital Münster, University of Münster, D-48149 Münster, Germany
[b] Department of Pathology, Anatomy and Cell Biology, and the Cancer Cell Biology and Signaling Program, Kimmel Cancer Center, Thomas Jefferson University, Philadelphia, PA, 19107, USA
[c] Department of Chemical and Biological Sciences, "Aurel Vlaicu" University of Arad, Romania and Mass Spectrometry Laboratory, National Institute for Research and Development in Electrochemistry and Condensed Matter, Timisoara, Romania

ARTICLE INFO

Available online 18 January 2014

Keywords:
Decorin
Dermatan sulfate
SLRP
Extracellular matrix
Fibroblast growth factor

ABSTRACT

Decorin is a small leucine-rich proteoglycan harboring a single glycosaminoglycan chain, which, in skin, is mainly composed of dermatan sulfate (DS). Mutant mice with targeted disruption of the decorin gene ($Dcn^{-/-}$) exhibit an abnormal collagen architecture in the dermis and reduced tensile strength, collectively leading to a skin fragility phenotype. Notably, Ehlers–Danlos patients with mutations in enzymes involved in the biosynthesis of DS display a similar phenotype, and recent studies indicate that DS is involved in growth factor binding and signaling. To determine the impact of the loss of DS-decorin in the dermis, we analyzed the glycosaminoglycan content of $Dcn^{-/-}$ and wild-type mouse skin. The total amount of chondroitin/dermatan sulfate (CS/DS) was increased in the $Dcn^{-/-}$ skin, but was overall less sulfated with a significant reduction in bisulfated ΔDiS2,X (X = 4 or 6) disaccharide units, due to the reduced expression of uronyl 2-O sulfotransferase (Ust). With increasing age, sulfation declined; however, $Dcn^{-/-}$ CS/DS was constantly undersulfated *vis-à-vis* wild-type. Functionally, we found altered fibroblast growth factor (Fgf)-7 and -2 binding due to changes in the micro-heterogeneity of skin $Dcn^{-/-}$ CS/DS. To better delineate the role of decorin, we used a 3D $Dcn^{-/-}$ fibroblast cell culture model. We found that the CS/DS extracts of wild-type and $Dcn^{-/-}$ fibroblasts were similar to the skin sugars, and this correlated with the lack of uronyl 2-O sulfotransferase in the $Dcn^{-/-}$ fibroblasts. Moreover, Ffg7 binding to total CS/DS was attenuated in the $Dcn^{-/-}$ samples. Surprisingly, wild-type CS/DS significantly reduced the binding of Fgf7 to keratinocytes in a concentration dependent manner unlike the $Dcn^{-/-}$ CS/DS that only affected the binding at higher concentrations. Although binding to cell-surfaces was quite similar at higher concentrations, keratinocyte proliferation was differentially affected. Higher concentration of $Dcn^{-/-}$ CS/DS induced proliferation in contrast to wild-type CS/DS. 3D co-cultures of fibroblasts and keratinocytes showed that, unlike $Dcn^{-/-}$ CS/DS, wild-type CS/DS promoted differentiation of keratinocytes. Collectively, our results provide novel mechanistic explanations for the reported defects in wound healing in $Dcn^{-/-}$ mice and possibly Ehlers–Danlos patients. Moreover, the lack of decorin-derived DS and an altered CS/DS composition differentially influence keratinocyte behavior.

1. Introduction

Decorin belongs to the family of the small leucine-rich proteoglycans (Iozzo and Murdoch, 1996) and is covalently linked with one glycosaminoglycan chain (GAG). Depending on the tissue decorin is covalently linked with either chondroitin or dermatan sulfate (CS/DS). Decorin is a multifunctional proteoglycan involved in several biological processes, like matrix organization (Seidler and Dreier, 2008), myogenesis (Brandan and Gutierrez, 2013), inflammation and cancer (Schaefer and Iozzo, 2008, 2012). The biosynthesis of GAGs is a multi-step process that begins with the formation of a specific carbohydrate–protein linkage region and continues with the alternating addition of D-glucuronic acid (D-GlcA) and either D-N-acetylglycosamine (D-GlcNAc) or D-N-acetylgalactosamine (D-GalNAc). CS/DS, the two types of galactosaminoglycans, is distinguished by the absence or presence of L-IdoA residues, respectively. The dermatan sulfate epimerase (*Dse*) together with several sulfotransferases modifies the CS/DS chain thus introducing a micro-heterogeneity along the chain. It is known that DS and CS show

Abbreviations: SLRP, small leucine-rich proteoglycan; $Dcn^{-/-}$, decorin-null mouse; GAG, glycosaminoglycan; DS, dermatan sulfate; CS, chondroitin sulfate; *Dcn*, mouse decorin gene; Fgf, fibroblast growth factor; ECM, extracellular matrix; EDS, Ehlers–Danlos syndrome; $Dse1^{-/-}$, dermatan sulfate epimerase 1-null mice.

☆ This work was financially supported by the German Society for Research (grant DFG SE1431/1-1) to DGS, GRK 1549 International Research Training Group 'Molecular and Cellular GlycoSciences' to KN and JR, and NIH grants CA39481 and CA47282 to RVI.

* Corresponding author. Tel.: +49 251 8355586; fax: +49 251 8355596.
E-mail address: dgseidle@uni-muenster.de (D.G. Seidler).

[1] These authors contributed equally.

0945-053X/$ – see front matter © 2014 Elsevier B.V. All rights reserved.
http://dx.doi.org/10.1016/j.matbio.2014.01.003

different biological functions (Sugahara et al., 2003) which is primarily due to a greater conformational flexibility of L-IdoA-containing GAGs (Inoue et al., 1990; Mulloy and Forster, 2000) and more frequently 2-O-sulfated than D-GlcA as the hexuronic acid moiety (Kobayashi et al., 1999). There are several DS proteoglycans and the most prominent in skin is decorin (Iozzo, 1997). Decorin contains about 60% L-IdoA in the dermis (Malmström et al., 2012) in contrast to the lack of L-IdoA in bone (Cheng et al., 1994). The lack of decorin in mice ($Dcn^{-/-}$) results in abnormal collagen fibrillogenesis and skin fragility (Danielson et al., 1997). Interestingly, tendons of $Dcn^{-/-}$ mice were less affected by aging compared to wild-type tendon (Dunkmann et al., 2013). The $Dcn^{-/-}$ mice however show a delayed epidermal wound closure and a significantly delayed dermal wound healing (Järveläinen et al., 2006). The loss of decorin and the impact on fibroblasts are well studied: $Dcn^{-/-}$ fibroblasts proliferate and adhere better compared to wild-type and express more β1 integrin (Ferdous et al., 2010). Addition of decorin proteoglycan but not decorin protein core can rescue the phenotype of fibrillar collagens (Seidler et al., 2005; Rühland et al., 2007) and the adhesive phenotype by reducing the amount of β1 integrin and stabilizing the vimentin intermediate filament system during matrix synthesis (Jungmann et al., 2012). These results indicate that the DS chain of decorin could also play a major role during regeneration and wound healing. This concept is further supported by studies utilizing $Dse1^{-/-}$ mice, which also exhibit heterogeneous collagen fibrils and skin fragility presumably as a consequence of reduced amount of L-IdoA in CS/DS of decorin and the disrupted L-IdoA clusters in the dermis (Maccarana et al., 2009). Consistent with these findings, reduced cell surface L-IdoA content of aortic smooth muscle cells leads to delayed wound healing and inability of directional migration (Bartolini et al., 2013), underlying the importance of DS in mediating proliferation, migration and adhesion (Malmström et al., 2012).

There are several mutations described in enzymes involved in the post-translational modifications of proteoglycans (Seidler, 2012). For example: mutation in the gene *B4GALT7*, an enzyme involved in the synthesis of the linkage region of GAGs leads to an Ehlers–Danlos syndrome with skin fragility and wound healing deficiency (Kresse et al., 1987; Faiyaz-Ul-Haque et al., 2004). Notably, the fibroblasts from the affected patients display defective biosynthesis of decorin characterized by release of decorin partially lacking a GAG chain (Kresse et al., 1987; Seidler et al., 2006) and reduced amount of L-IdoA in the partially processed GAG (Seidler et al., 2006). Mutations in *CHST14*, the gene that encodes the dermatan-4-O sulfotransferase, leads to an Ehlers–Danlos syndrome categorized either as EDS Kosho-type or kyphoscoliosis-type with a delayed wound healing (Miyake et al., 2010; Shimizu et al., 2011). The loss of DS in the dermis leads to abnormal fibrillar collagen due to the defects in post-translational modifications of decorin (Miyake et al., 2010; Shimizu et al., 2011).

Growth factors require GAGs for their function (Sarrazin et al., 2011) and DS can affect interferon-γ (Fernandez-Botran et al., 1999; Bocian et al., 2013) and fibroblast growth factors (FGFs) (Trowbridge and Gallo, 2002; Taylor et al., 2005). In a contact allergy model, loss of decorin leads to a reduced edema formation due to a disturbed cytokine and chemokine expression profile (Seidler et al., 2011). Wound fluid contains GAGs, and the DS derived from wound fluid promotes FGF2 signaling (Penc et al., 1998). Indeed, oligosaccharides derived from skin fibroblast DS decorin can bind FGF2 (Zamfir et al., 2003). FGF7-induced proliferation is DS dependent (Trowbridge and Gallo, 2002). However, the specificity of DS interaction with growth factor is still debated. Recently, it has been shown that FGFs display a clear preference for distinct structural features of heparin (Xu et al., 2012). Therefore, the delayed wound healing of $Dcn^{-/-}$ mice could partially occur due to the lack of DS in skin resulting in an altered Fgf7 function on keratinocytes.

In this study, we investigated the impact of the loss of DS of decorin in skin on growth factor binding. We found that the CS/DS chains of decorin null skin were uniformly undersulfated and this affected the binding and potentially, the biological activity of various Fgfs. Interestingly, only Fgf2 and Fgf7 binding to CS/DS was affected by the reduced amount of sulfation. Using a co-culture system of keratinocytes grown on the top of fibroblasts embedded in their own 3D matrix, we discovered that the absence of decorin caused a delay in differentiation. Our findings offer novel mechanistic explanations for the established defects in wound healing in $Dcn^{-/-}$ mice and possibly Ehlers–Danlos patients.

2. Results

2.1. $Dcn^{-/-}$ dermal CS/DS was undersulfated due to the reduced amount of ΔDi2,XS (X = 4 or 6) and ΔDi2S

Dorsal skin from male wild-type and $Dcn^{-/-}$ mice at postnatal age of 30, 45 and 75 (pools of 3–5 mice) was extracted and analyzed for total and highly-sulfated CS/DS content. $Dcn^{-/-}$ P30 mice showed significantly more uronic acid compared to the respective wild-type mice (data not shown). The values are referring to the wet weight of the skin. Analysis of highly-sulfated CS/DS obtained with further fractionation by HPLC-DEAE (Zamfir et al., 2009) showed significantly higher amount of uronic acid in P30 $Dcn^{-/-}$ mice highly-sulfated CS/DS compared to wild-type mice (Fig. 1A; n = 3; $^{**}P < 0.01$), and a concurrent significant reduction in the total sulfate content (Fig. 1B; n = 3; $^{**}P < 0.01$). With aging, both genotypes showed similar amounts of uronic acid (Fig. 1A); however, the $Dcn^{-/-}$ mice displayed reduced sulfation (Fig. 1B). The content of CS/DS GAGs in wild-type is similar to the amount described for rat skin (Jung et al., 1997) and the amount of highly-sulfated CS/DS for the decorin extraction in porcine skin (Zhao et al., 2013).

Disaccharide analysis of highly-sulfated CS/DS revealed that wild-type P30 CS/DS contained 6 differentially-sulfated disaccharides in contrast to $Dcn^{-/-}$ GAGs which contained only 4 differentially-sulfated disaccharides. In both genotypes, ΔDi4S and ΔDi6S were present to a similar extent at P30. The minor modification of ΔDi2S was detectable by FACE analysis in only one out of three CS/DS extractions in $Dcn^{-/-}$ skins. For wild-type CS/DS always contained detectable amounts of 2-O sulfated disaccharides. Our method could not distinguish between the disulfated ΔDiS2,4 and ΔDiS2,6 species, therefore we used Di2,XS (X = 4 or 6). In line with ΔDiS2, ΔDiS2,X (X = 4 or 6) was also not detectable in $Dcn^{-/-}$ CS/DS in contrast to wild-type CS/DS (Fig. 1C, D). The presence of ΔDiS2,4 was confirmed by MS/MS fragmentation of wild-type chondroitin ACI lyase digested CS/DS disaccharides (Supplementary Fig. 1). To confirm the reduction in 2-O-sulfation, we analyzed the expression of the respective enzyme in dermal extracts and fibroblasts: uronyl 2-O sulfotransferase (Ust) (Fig. 1E, F). In vivo the Ust expression was reduced in $Dcn^{-/-}$ skin extracts (Fig. 1E, upper panel). Lower panel shows the total protein stain of the extracts. Furthermore, immune blots revealed similar Ust protein expression in primary mouse wild-type and 3T3 fibroblasts; however, $Dcn^{-/-}$ fibroblasts were negative for Ust (Fig. 1F; n = 3). Therefore, the loss of decorin in the murine dermis leads to changes in uronic acid and sulfate content of highly-sulfated CS/DS GAGs.

Next, we determined the DS content of highly-sulfated CS/DS samples following chondroitin ACI lyase digestion and separation on a Superdex column (Zamfir et al., 2003). We found no difference in the amount of disaccharides derived from wild-type or $Dcn^{-/-}$ CS/DS (11–15%). However, P30 $Dcn^{-/-}$ samples contained about twice the proportion of tetrasaccharides as wild-type contained (65% vs 35% Table 1) and about thirteen fold lower hexasaccharides (~3% vs 40%, Table 1 (analysis of 6 pooled skin extracts)). The lack of DS from decorin not only displays differences in composition of the disaccharide structures but also affects oligosaccharide structures. Binding of growth factors to CS/DS also required a certain size of L-IdoA-blocks (Malmström et al., 2012). These results suggest that $Dcn^{-/-}$ CS/DS displays changes in

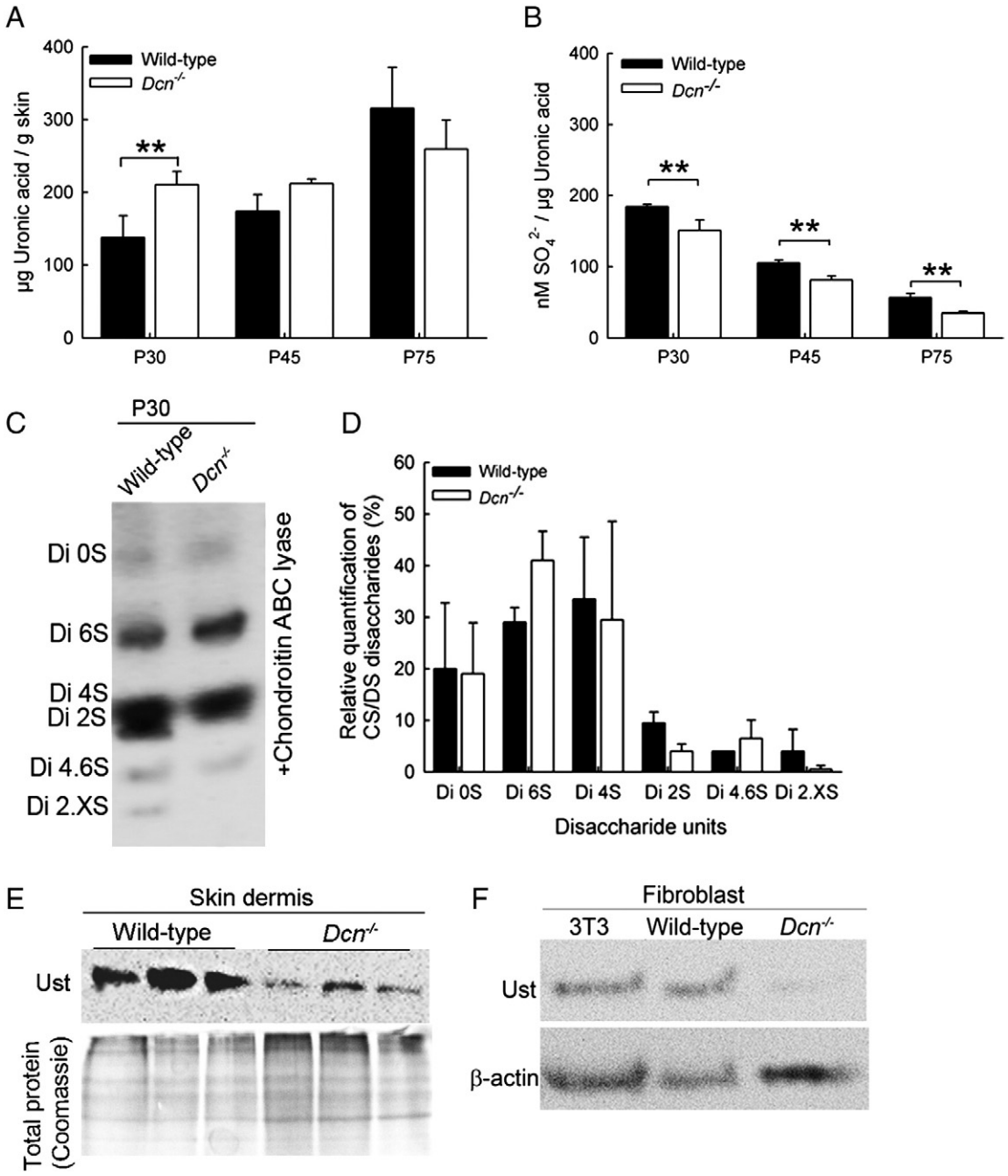

Fig. 1. Characterization of skin CS/DS at different stages of wild-type and $Dcn^{-/-}$ mice. GAGs were isolated from the back of adult male mice skin at different postnatal stages (P30, P45 and P75) and analyzed for uronic acid and sulfate content of highly-sulfated CS/DS fractions (A and B). (A) Uronic acid content in the wild-type and $Dcn^{-/-}$ highly-sulfated CS/DS extracts at different stages (n = 3; $^{**}P < 0.01$). (B) The sulfate content of P30, P45 and P75 highly-sulfated fractions of CS/DS of wild-type and $Dcn^{-/-}$ GAGs (n = 3; $^{**}P < 0.01$). (C) Disaccharide analysis of the highly-sulfated fractions of CS/DS of wild-type and $Dcn^{-/-}$ GAGs derived from P30 and P45. GAGs were digested with chondroitin ABC lyase followed by AMAC labeling and separation by FACE-PAGE. (D) Quantification of the disaccharide composition was analyzed by ImageJ software (n = 3; each 5–6 pooled skin). (E) Immune blot for uronyl 2-O sulfotransferase (Ust) protein expression in wild-type and $Dcn^{-/-}$ newborn dermal extracts. (F) Immune blot for uronyl 2-O sulfotransferase (Ust) protein expression in wild-type and $Dcn^{-/-}$ fibroblasts. As a positive control, 3T3 mouse fibroblasts were used with β-actin as a loading control (n = 3).

Table 1
Highly-sulfated CS/DS P30 GAGs purified from $Dcn^{-/-}$ and wild-type mice — Chondroitin ACI lyase digested highly-sulfated $Dcn^{-/-}$ and wild-type CS/DS GAGs were fractioned on a Superdex Peptide column. The column was calibrated with cytochrome C to determine V_0 and glycin to determine V_t. Data represent CS/DS of 6 pooled skins.

Fraction	Wild-type [%]	$Dcn^{-/-}$ [%]
V_0	14	17
Disaccharide	11	15
Tetrasaccharide	35	65
Hexasaccharide	40	3

the size of blocks, which therefore might have an altered growth factor binding.

Binding of growth factors to CS/DS oligosaccharides requires not only existence of particular sulfation motifs, but also presence of L-IdoA-blocks with certain size (Malmström et al., 2012). The loss of decorin in the murine dermis leads to changes in uronic acid and sulfate content of highly-sulfated CS/DS GAGs, with deletion of 2-O sulfated motifs in the CS/DS chain. Furthermore, $Dcn^{-/-}$ CS/DS displays changes in the size of the blocks, which therefore might have an altered growth factor binding.

2.2. Differential binding of growth factors to galactosaminoglycans extracted from mouse skin

To demonstrate a functional consequence of the altered sulfation, we performed solid-phase binding assays with various murine Fgfs. Recombinant fusion proteins harboring Fgf1, Fgf7 or Fgf8 fused to alkaline phosphatase (Herzog et al., 2011) were generated as soluble ligand, using HEK293 cells. Decorin derived from skin fibroblasts with 50–55% IdoA content (Seidler et al., 2006) served as a positive control. For soluble AP no binding was observed to bovine serum albumin, decorin or the wild-type and $Dcn^{-/-}$ CS/DS. AP-Fgf1, AP-Fgf7 and AP-Fgf8 showed similar binding to control decorin and minimal binding to bovine serum albumin (Fig. 2A). AP-Fgf1 showed only weak binding to highly-sulfated CS/DS extracted from P30, P45 and P75 skin of either wild-type or $Dcn^{-/-}$ mice indicating that the micro-heterogeneity of the GAGs was not important for Fgf1 binding. However, AP-Fgf1 binding to the positive control decorin was observed (Herzog et al., 2011). In contrast, AP-Fgf7 and AP-Fgf8 had higher binding capacity to wild-type and $Dcn^{-/-}$ CS/DS compared to Fgf1 (Fig. 2A; n = 3; $^{*}P < 0.05$). At P30 and P45 AP-Fgf7 binding was significantly higher in wild-type compared to $Dcn^{-/-}$ GAGs (n = 3; $^{*}P < 0.05$). At P75 there was no difference in Fgf7 binding anymore.

To analyze the influence of sulfation, the binding of AP-Fgf7 was interfered with different NaCl concentrations. P30 $Dcn^{-/-}$ highly-sulfated CS/DS AP-Fgf7 complex was more stable compared to wild-type. However, at stage P45 there was no difference in the stability of AP-Fgf7/wild-type or $Dcn^{-/-}$ CS/DS (data not shown). Another growth factor important in wound healing of the skin is Fgf2 (for review: Werner and Grose, 2003). Digoxigenin-labeled human FGF2 (Dig-FGF2) was used for the binding assay. The Dig-FGF2 bound to control decorin to the same extent and minimally to bovine serum albumin (Fig. 2B) as AP-fusion proteins. Interestingly, the binding of Dig-FGF2 was at all time points significantly reduced in the $Dcn^{-/-}$ undersulfated preparations (Fig. 2B; n = 2; $^{*}P < 0.05$), indicating that FGF2 function could also be affected in $Dcn^{-/-}$ mice.

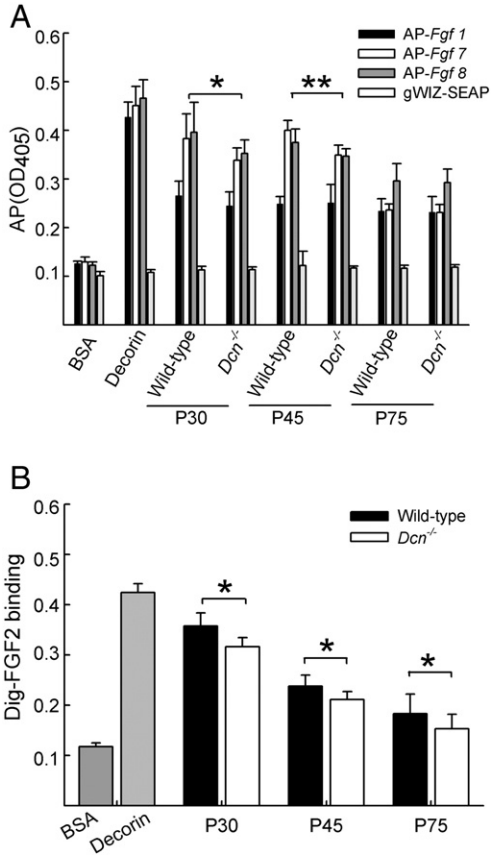

Fig. 2. AP-Fgf fusion proteins and their binding to highly-sulfated CS/DS from wild-type and $Dcn^{-/-}$ skin. Mouse alkaline phosphatase tagged growth factors (AP-Fgf1, AP-Fgf7 and AP-Fgf8) and AP (gWIZ-SEAP) alone were incubated with immobilized mouse skin highly-sulfated CS/DS GAGs derived from different stages (P30, 45, 75). (A) Binding of AP, AP-Fgf1, AP-Fgf7 and AP-Fgf8 was evaluated by alkaline phosphatase assay, using 1% BSA as a negative and decorin derived from conditioned medium of skin fibroblasts (Herzog et al., 2011) as a positive control (mean ± SD; n = 3; Mann–Whitney test; $^{*}P < 0.05$; $^{**}P < 0.01$). (B) FGF2 binding was determined with GAG extracts derived from P30, P45 and P75 using digoxigenin labeled FGF2 (Dig-FGF2) detected by alkaline phosphatase assay. 1% BSA was used as a negative and decorin derived from conditioned medium of skin fibroblasts as a positive control (mean ± SD; n = 2; $^{*}P < 0.05$).

2.3. DS proteoglycan expression under 3D culture conditions for wild-type and $Dcn^{-/-}$ fibroblasts

To establish the role of SLRPs, we determined the expression of biglycan and decorin in wild-type fibroblast 3D cultures (Seidler et al., 2005; Rühland et al., 2007; Jungmann et al., 2012). There was a dynamic change in the expression of decorin mRNA in wild-type fibroblasts during the time course from 2 to 10 days (Fig. 3A). At day 4, a significant (~6-fold) increase of decorin expression was observed. At day 6, when cells synthesized and deposit collagen in the ECM, there was still a 5-fold increase of decorin expression. This further declined until day 8. At day 10, when the ECM is formed around the fibroblasts, there was another burst of decorin mRNA synthesis (Fig. 3A). As expected, the amount of decorin proteoglycan, a broad band centered at ~100 kDa, progressively accumulated in the cell/matrix extracts (Fig. 3B, top panel); β-actin is shown as a loading control (Fig. 3B, bottom panel). The preferential increase of decorin SLRP in these 3D cultures suggests that the loss of DS decorin could be the candidate moiety affecting sulfation. Indeed, we found no compensatory changes in biglycan mRNA synthesis from the $Dcn^{-/-}$ fibroblasts for up to 10 days (Fig. 3A).

Next, we analyzed the composition of CS/DS from 3D fibroblast cultures to study the impact of DS decorin on CS/DS in this system. The 14-day extracts of wild-type, $Dcn^{-/-}$ fibroblasts and $Dcn^{-/-}$ fibroblasts treated with decorin showed that $Dcn^{-/-}$ fibroblasts contained similar amounts of uronic acid compared to wild-type; however, a slight increase was observed for $Dcn^{-/-}$ extracts alike observed in vivo (Fig. 3C; n = 3–4). The total sulfate content was 40% less compared to the wild-type fibroblasts, consistent with the in vivo results and could be increased by addition of decorin the $Dcn^{-/-}$ fibroblast (Fig. 3D). Cell lysates of wild-type and $Dcn^{-/-}$ fibroblasts showed that Ust protein expression is affected by the loss of decorin (Fig. 1F). This confirms the results obtained in vivo, where $Dcn^{-/-}$ mice display an overall reduction in content compared to wild-type. Exogenous treatment with decorin of $Dcn^{-/-}$ fibroblasts can partially rescue the total amount of sulfation in this system.

2.4. CS/DS of wild-type and $Dcn^{-/-}$ fibroblasts and their binding capacity for AP-Fgfs

To determine the possible functional difference of the CS/DS extracted from 3D fibroblast cultures, we performed AP-Fgf binding experiments. We discovered that the binding capacity of AP-Fgf1 to $Dcn^{-/-}$ and $Dcn^{-/-}$ + decorin GAGs compared to the decorin control was lower (data not shown). The results for AP-Fgf1 confirm previous studies with no impact of DS on Fgf1 function (Trowbridge and Gallo, 2002). Soluble AP (gWIZ-SEAP) control did not bind to the growth factors. Interestingly, AP-Fgf8 bound to a similar extent to the total CS/DS extracts, albeit to a lower extent when compared to decorin (Fig. 3E). In contrast to the binding of AP-Fgf8 to either wild-type or $Dcn^{-/-}$ fibroblast total CS/DS, AP-Fgf7 binding was significantly higher in wild-type fibroblast CS/DS compared to $Dcn^{-/-}$ (n = 3; $^{**}P < 0.01$). Interestingly, total CS/DS of $Dcn^{-/-}$ 3D cultures supplemented for 14 days with DS decorin showed also significantly increased binding of AP-Fgf7 (Fig. 3E; n = 3; $^{*}P < 0.05$) indicating that exogenous decorin

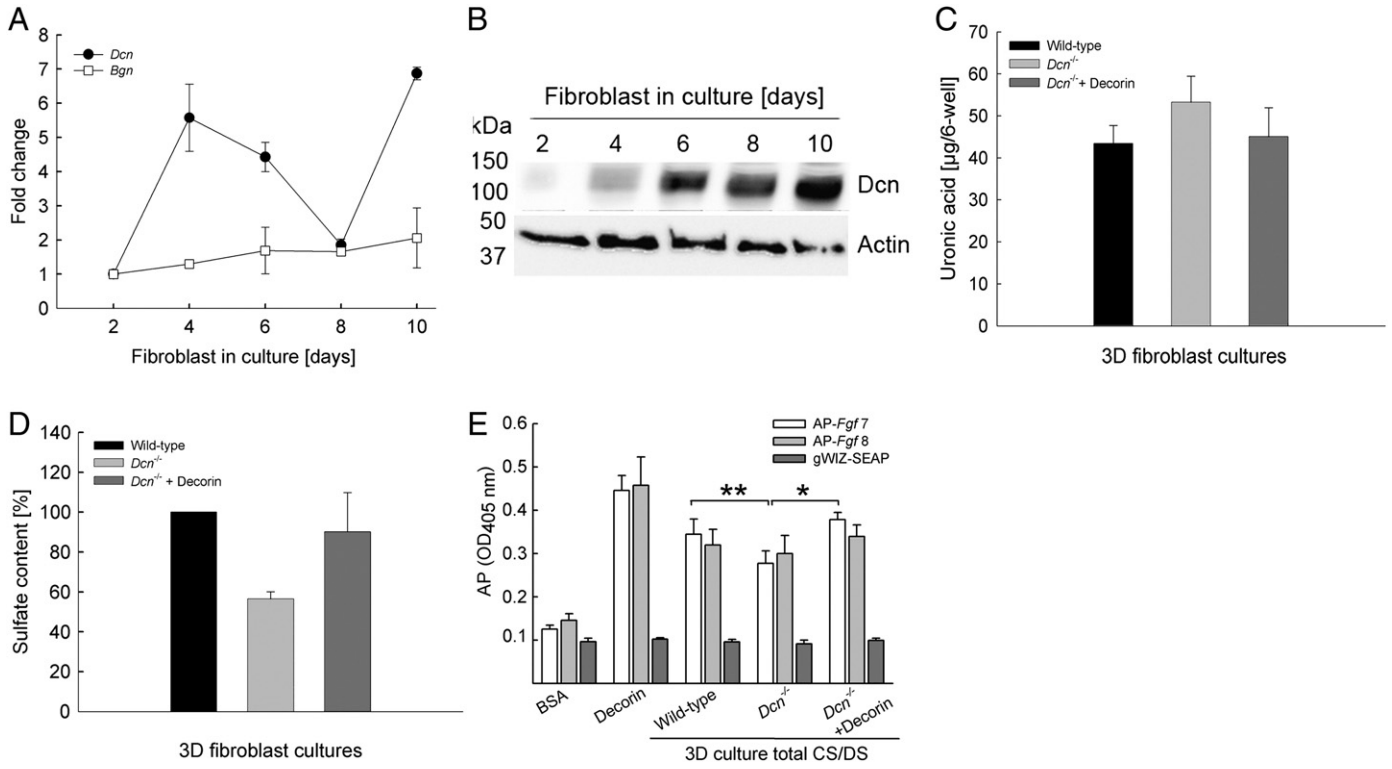

Fig. 3. CS/DS characterization in 3D fibroblasts cultures. (A) Decorin (*Dcn*) and biglycan (*Bgn*) expression was determined with qRT-PCR using cDNA derived from 3D cultures of wild-type fibroblasts harvested at different time points. Ubiquitin c was used as an endogenous control. (B) Western blots of wild-type fibroblasts cultured for 2–10 days in the presence of ascorbate-2 phosphate using LF113 antibody (gift from Larry Fisher) to detect decorin (top panel) and β-actin as a loading control (bottom panel). (C) Total CS/DS extracts of $Dcn^{-/-}$, $Dcn^{-/-}$ + decorin and wild-type fibroblasts were cultured for 14 days in the presence of ascorbate-2 phosphate. Total CS/DS extracts of 3D cultures were analyzed for uronic acid (n = 3; each 2–3 pooled 6-wells). (D) Total sulfate content of the 3D culture CS/DS extracts (n = 3; each 2–3 pooled wells). (E) Solid-phase binding assay of alkaline phosphatase tagged growth factors (AP-Fgf7 and AP-Fgf8) and total CS/DS extracted from 3D cultures. gWIZ-SEAP was used as a negative control. Decorin derived from conditioned medium of skin fibroblasts was used as a positive control. Data are expressed as mean ± SD of three experiments performed in duplicates with each 2–3 pooled 6-well plates of 3D cell cultures (number of experiments: n = 3; $^{*}P < 0.05$; $^{**}P < 0.01$).

can rescue the phenotype. The binding of AP-Ffg8 was still not affected (Fig. 3E). The binding assays for mouse skin and 3D fibroblast CS/DS from wild-type and $Dcn^{-/-}$ origin revealed that the structural differences of these GAGs influenced their binding capacity to Fgf7. Keratinocytes are the dominant Fgf7 responding cells in the skin (Werner et al., 2007) and therefore the influence of CS/DS and Fgf7 on keratinocytes was analyzed.

2.5. Influence of wild-type and $Dcn^{-/-}$ CS/DS on primary keratinocyte proliferation

As Fgf7 and DS are involved in keratinocyte proliferation and migration during wound healing (Taylor et al., 2005), we evaluated the impact of AP-Fgf7 binding to keratinocytes in the presence of exogenous P30 wild-type and $Dcn^{-/-}$ CS/DS. Interestingly, wild-type and $Dcn^{-/-}$ CS/DS significantly reduced the binding of AP-Fgf7 in a concentration dependent manner (n = 3; $^{**}P < 0.01$; $^{***}P < 0.001$), indicating that the soluble skin GAGs can capture the Fgf7 even in the presence of cell surface heparan sulfate (Fig. 4A). At a low concentration (0.1 µg/ml) the less sulfated $Dcn^{-/-}$ CS/DS significantly increased the amount of cell-surface bound AP-Fgf7 compared to wild-type CD/DS treated cells (n = 3; $^{*}P < 0.05$). In higher concentrations this difference was not present any longer.

For the functional impact of the human FGF7/GAG interaction we analyzed human primary keratinocyte proliferation. Primary human keratinocytes were cultured to a density of 40–60% and afterwards medium was changed to MCDB 153 medium supplemented with 5 ng/ml FGF7 or FGF7 + CS/DS (different concentrations) for 24 h + 16 h to induce proliferation. The proliferation is lower compared to previously published data because we incubated the human keratinocytes for 16 h in the presence of BrdU in contrast to 72 h incubation time (Trowbridge and Gallo, 2002), taking as an advantage that only newly synthesized cells are detected with BrdU incorporation. Keratinocytes proliferation in the presence of 5 ng/ml FGF7 and different GAG concentrations was only partially influenced (Fig. 4B). There was a slightly positive influence with 0.1 and 1 µg/ml $Dcn^{-/-}$ CS/DS + FGF7 on keratinocyte proliferation in contrast to wild-type CS/DS. Interestingly, 5 µg/ml $Dcn^{-/-}$ CS/DS and FGF7 again induced significantly cell proliferation of up to 60% when compared to FGF7/wild-type CS/DS or FGF7 alone (n = 6; $^{***}P < 0.001$, $^{**}P < 0.01$) treated keratinocytes. These results indicate that the decreased binding of FGF7 to the cell surface in the presence of wild-type GAGs prevented proliferation; however, for $Dcn^{-/-}$ CS/DS proliferation was observed. Next, we analyzed the different highly-sulfated CS/DS on keratinocyte proliferation alone. 40–60% confluent primary human keratinocytes were incubated with MCDB 153 medium, supplemented with different concentrations of wild-type or $Dcn^{-/-}$ highly-sulfated CS/DS. As a positive control for proliferation, the Celloneer® culture medium was used. Proliferation was determined by BrdU incorporation as described above. CS/DS preparations isolated from both genotypes had a minor, but similar impact on proliferation at low dosage (0.001–0.05 µg/ml, equivalent to 22–111 pM) (Fig. 4C). However, at higher (more physiological) concentrations, the CS/DS preparation from the decorin-null mice induced keratinocyte cell proliferation up to 100% in contrast to the wild-type preparations (Fig. 4C; n = 7, $^{**}P < 0.01$). No differences in the viability or metabolic activity of the cells were detected for all tested GAG concentrations with MTT assays (data not shown). Thus, undersulfated CS/DS derived from decorin-null mice, which display a reduced 2-O sulfation, can stimulate keratinocyte proliferation. To exclude growth factor contaminations CS/DS preparations were analyzed at 280 nm

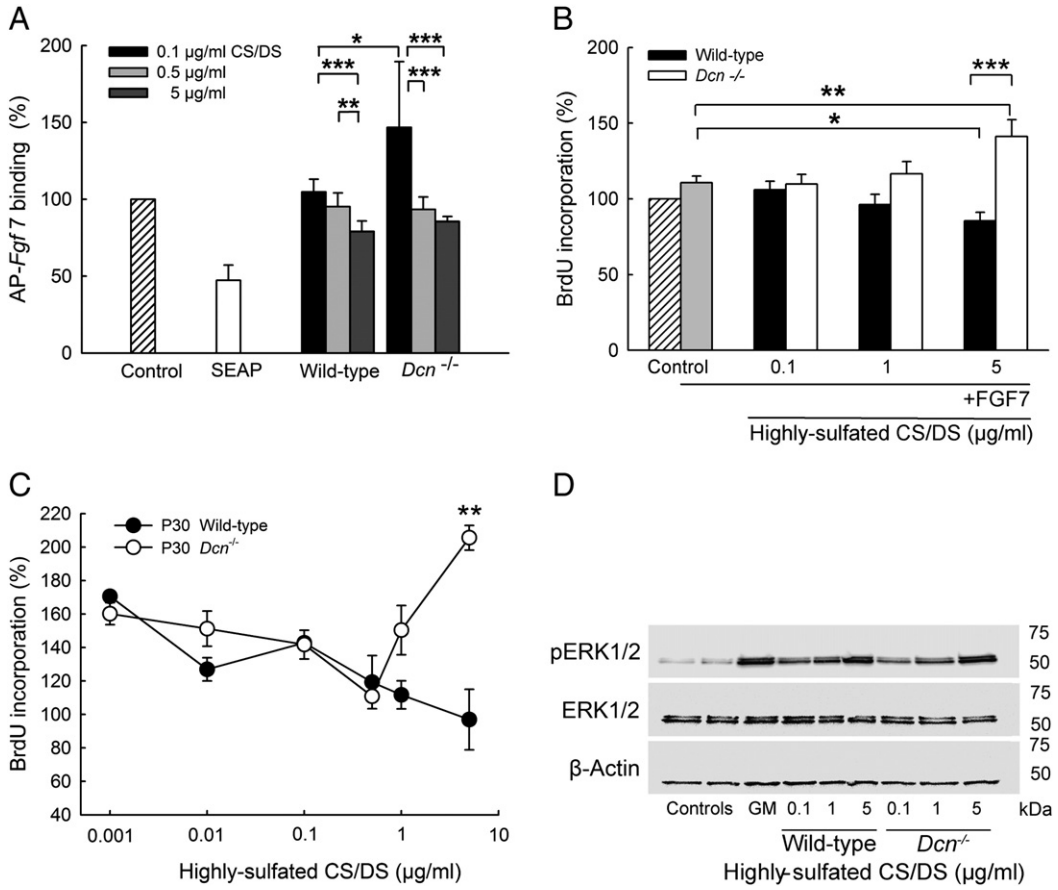

Fig. 4. Binding properties and functional impact of FGF7 and GAGS on keratinocytes. (A) Binding of AP-Fgf7 to the cell surfaces of human primary keratinocytes in the presence of 0.1, 0.5 and 5 µg/ml CS/DS purified from wild-type and $Dcn^{-/-}$ P30 skin (data are expressed as mean ± SD: n = 3; $^{*}P < 0.05$; $^{**}P < 0.01$; $^{***}P < 0.001$). Conditioned medium of gWIZ-SEAP expressed in HEK 293 cells was used as a negative control (SEAP). (B) Proliferation of human primary keratinocytes in the presence of 0.1, 1 and 5 µg/ml wild-type and $Dcn^{-/-}$ P30 CS/DS and 5 ng/ml FGF7 (data are expressed as mean ± SEM: n = 5–6 independent experiments performed in triplicate; $^{*}P < 0.05$; $^{**}P < 0.01$; $^{***}P < 0.001$). (C) Dose response proliferation curve of human primary keratinocytes treated with highly-sulfated wild-type and $Dcn^{-/-}$ CS/DS (after β-elimination) determined by 16 h BrdU incorporation. Data are expressed as mean ± SD of one representative experiment performed in triplicate and normalized to the control (number of experiments: n ≥ 3; statistics for 5 µg/ml: n = 7; $^{**}P < 0.01$). For statistical analysis Mann–Whitney test was used. (D) Influence of wild-type and $Dcn^{-/-}$ P30 highly-sulfated CS/DS GAGs on ERK1/2 activation. Keratinocytes were treated with 0.1, 1 and 5 µg/ml GAGs for 30 min and harvested with lysis buffer. 20 µg protein was analyzed by immune blotting for pERK1/2 and ERK1/2 protein expression. β-Actin was used as a loading control. Basal pERK1/2 expression was determined in non-treated keratinocytes and Celloneer® growth medium (GM) treated cells were used as a positive control.

UV. To evaluate the impact of CS/DS on keratinocyte proliferation we analyzed the activation of mitogen-activated kinase/extracellular regulated kinase-1,2 (ERK1,2) (Trowbridge and Gallo, 2002). Interestingly, for both wild-type and $Dcn^{-/-}$ CS/DS we could observe a concentration dependent (0.1–5 µg/ml) increase in ERK activation (Fig. 4D; n = 3). This result is indicating that both wild-type and $Dcn^{-/-}$ CS/DS induce ERK signaling. However, this affects keratinocytes differently, because only the $Dcn^{-/-}$ CS/DS induced proliferation in contrast to wild-type CS/DS. ERK activation is also known to be involved in differentiation.

2.6. Co-cultures of 3D fibroblasts and keratinocytes

To analyze keratinocyte behavior in a more in vivo-like situation, where keratinocytes are able to differentiate, we used a 3D model of fibroblasts embedded in their own collagen-rich matrix (Seidler et al., 2005; Stock et al., 2011) upon which keratinocytes are grown. The keratinocytes grew as multi-layer cells positive for the wide spectrum keratin marker pan-keratin (Fig. 5A). Collagen I staining was used to visualize the underlying fibroblast matrix. To exclude proliferative differences, we used low concentrations (0.1 µg/ml) of exogenous GAGs derived from P30 wild-type or $Dcn^{-/-}$ CS/DS for up to 72 h. As shown in figure Fig. 4D, both activated ERK to a similar extent. To determine the impact of CS/DS on keratinocyte differentiation, the co-cultures were analyzed for specific markers (Fig. 5B). Pan keratin was used as a general marker for keratinocytes seeded on wild-type 3D fibroblast matrices. In all three conditions, pan keratin was detectable. Quantification of the signal intensity per keratinocyte area showed that $Dcn^{-/-}$ CS/DS treated cultures expressed less pan keratin compared to wild-type treated cultures (Fig. 5C), indicating delayed differentiation (n = 19 images each condition; $^{***}P < 0.001$). The signal intensity of wild-type treated and untreated cultures was similar. Cytokeratin 10, a marker of early differentiation, was not differentially affected by the highly-sulfated CS/DS treatment (n = 19 images for the control and n = 25 for the treated cultures). The later differentiation marker involucrin, however, was reduced by $Dcn^{-/-}$ CS/DS treatment (Fig. 5B, C) (n = 19 images for the control and n = 27 for the treated cultures; $^{**}P < 0.01$). These results were supported by immune blotting of extracts of the 3D co-culture systems treated with wild-type or $Dcn^{-/-}$ CS/DS and the respective control (Fig. 5D). Signals were normalized to the loading control of human β-actin (Fig. 5D, left panel). Immune blots confirmed the significant reduction of involucrin in the $Dcn^{-/-}$ treated cultures compared to wild-type and the controls (Fig. 5D right panel; n = 3; $^{*}P < 0.05$).

These data confirm the impact of GAG sulfation on keratinocytes and could provide an explanation for the delayed wound healing in $Dcn^{-/-}$ mice (Järveläinen et al., 2006).

3. Discussion

The dermatan sulfate moiety in proteoglycans, such as decorin, mediates biological functions including extracellular matrix organization,

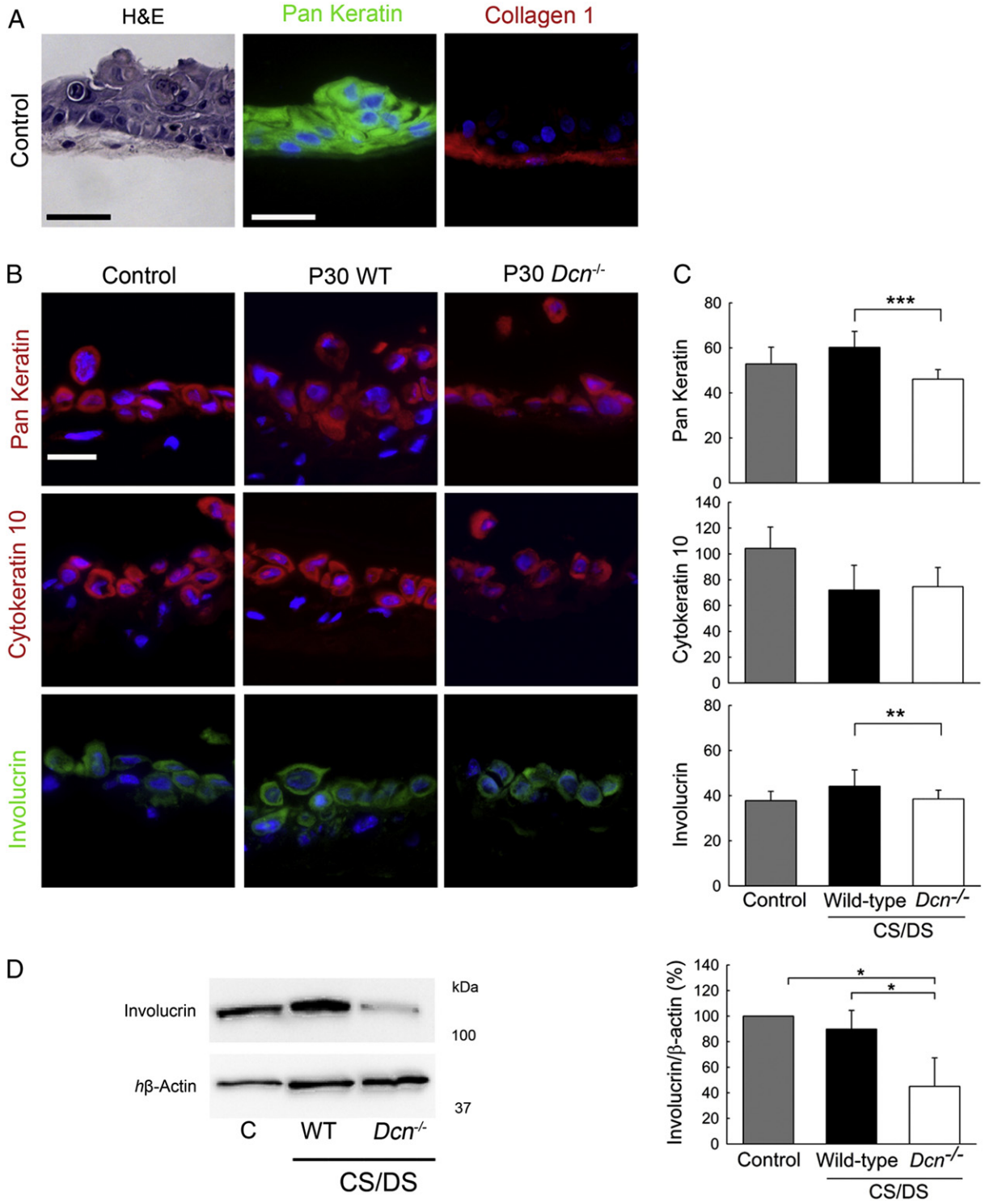

Fig. 5. Characterization of co-cultures of 3D wild-type fibroblasts and human primary keratinocytes. Keratinocytes were seeded on 3D fibroblast cultures for 24 h following an incubation for 72–144 h. (A) Keratinocytes were visualized by hematoxylin and eosin (H&E) (bar = 50 μm) and by immune fluorescence using the keratinocyte marker pan keratin (green) and collagen I (red) staining of the fibroblast matrix. (B) Differentiation of keratinocytes on 3D cultures treated with 0.1 μg/ml P30 wild-type and $Dcn^{-/-}$ highly-sulfated CS/DS monitored with markers: pan keratin (red), cytokeratin 10 (red) and involucrin (green). Fluorescence signals of pan keratin (n = 19 images for each condition), cytokeratin 10 (n = 19 images for the control and n = 25 for the treated cultures) and involucrin (n = 19 images for the control and n = 27 for the treated cultures) were quantified (C) and normalized on the area of stained keratinocytes. Data are expressed as mean ± SD (**$P < 0.01$; ***$P < 0.001$). (D) The fluorescence analysis was supported by immune blotting of co-culture protein extracts as described in (B). Left panel: Representative blot of 4.2 μg protein lysates stained for involucrin and human β-actin (hβ-actin). Right panel: the quantification of 3 different experiments expressed as mean ± SD (*$P < 0.05$; Student's t-test).

cell proliferation, migration and adhesion (Malmström et al., 2012; Seidler, 2012). We show for the first time, that a DS-decorin deficient matrix displays altered sulfate levels that affect growth factors involved in wound healing. The physiological importance of DS became obvious in the connective tissue disorder, Ehlers–Danlos syndrome (EDS), a group of inherited disorders characterized by cutis laxa, loose joints

and an altered wound healing. Minor subgroups of patients exhibit mutations in the *CHST14* or *B4GALT7* gene, encoding enzymes involved in DS synthesis (Kresse et al., 1987; Seidler et al., 2006; Miyake et al., 2010; Shimizu et al., 2011). Interestingly, in skin the major proteoglycan affected by the mutations of *CHST14* or *B4GALT7* is decorin because of its relatively high expression in fetal dermis (Scholzen et al., 1994). *CHST14* encodes the dermatan-4 sulfotransferase-1, and loss of function leads to the complete loss of DS in the dermis and to defects in collagen bundles (Miyake et al., 2010). Mutation in *B4GALT7* gene leads to a reduced activity of the galactosyltransferase 1 and the partial loss of the GAG chain of decorin (Kresse et al., 1987) and to a reduced L-IdoA content in decorin and biglycan (Seidler et al., 2006). Mutant mice with targeted disruption of the decorin gene exhibit also an abnormal collagen architecture in the dermis and reduced tensile strength, which together lead to a skin fragility phenotype (Danielson et al., 1997) and delayed healing of epidermal and significantly of dermal wounds (Järveläinen et al., 2006). In this study we discovered that loss of DS decorin is associated with subtle, but reproducible, changes in the GAG composition of the skin, mainly characterized by a reduced overall sulfation of CS/DS up to 75 days of postnatal life. For wild-type mice the extracted uronic acid amount from skin is comparable to previous studies in rat as well as the finding of reduced sulfation with aging (Jung et al., 1997). A more detailed study revealed that the content of porcine skin decorin GAG was 0.1–0.12 mg/g wet skin (Zhao et al., 2013). Particularly prominent is a reduction in ΔDi2,XS (X = 4 or 6) and ΔDi2S in $Dcn^{-/-}$ highly-sulfated CS/DS disaccharide structures. Sequence analysis of porcine skin decorin GAG revealed about 2.2% of Di2,4S-units (Zhao et al., 2013), supporting our hypothesis that the lack of DS decorin leads to the loss of specific functional GAG structures. These posttranslational changes may likely lead to loss of binding motifs for growth factors, like Fgf2 (Zamfir et al., 2003) and Fgf7 (Taylor et al., 2005).

We further noticed that with aging, total sulfation is further reduced within both wild-type and $Dcn^{-/-}$ GAGs; however, $Dcn^{-/-}$ GAGs are constantly less sulfated than wild-type. CS/DS from wild-type and $Dcn^{-/-}$ skin shows a different composition, like the CS/DS of the 3D fibroblast cell culture. Notably, the reduced sulfation in highly-sulfated $Dcn^{-/-}$ CS/DS correlates well with a reduction in uronyl-2-O sulfotransferase expression in fibroblasts. Interestingly, at P45, 2-O-sulfation is still detectable but reduced compared to $Dcn^{-/-}$ GAGs. At P75 ΔDi2S is not detectable anymore. Interestingly, the partial loss of the decorin GAG chain in EDS patient affects the amount of L-IdoA in decorin and biglycan (Seidler et al., 2006). Thus, we hypothesized that some defects could be due to structural alterations of CS/DS of these patients. This could explain the heterogeneous clinical picture and the difficulties in diagnosing these patients, because the symptoms are changing with age (Shimizu et al., 2011).

Growth factors are involved in wound healing and the reduced amount of ΔDi2,4S and ΔDi2S in CS/DS could affect the signaling of Fgf as shown for heparin (Ashikari-Hada et al., 2009). Thus, changes in the micro-heterogeneity of $Dcn^{-/-}$ P30 CS/DS could lead to a reduced Fgf7 and Fgf2 binding in contrast to Fgf1 or Fgf8. Previously it has been shown that growth factors display a preference for specific HS oligosaccharides (Xu et al., 2012). The reduced Fgf2 binding to $Dcn^{-/-}$ CS/DS could explain the increased proliferation of $Dcn^{-/-}$ embryonic fibroblasts (Ferdous et al., 2010). The role of CS/DS sulfation pattern in wound healing is not fully understood. For the healing dermis, changes in CS/DS structures or the loss of CS/DS of decorin causes alterations in the ECM and cell/matrix interactions (Rühland et al., 2007; Jungmann et al., 2012). $Dse1^{-/-}$ mice contain only 25% L-IdoA in the dermis and also show an altered ECM (Maccarana et al., 2009), however there are so far no data about skin wound healing. In vitro, wound healing of aortic smooth muscle cells derived from $Dse1^{-/-}$ mice was delayed due to a reduced cell surface L-IdoA. The functional consequence was the loss of directional migration of these cells (Bartolini et al., 2013). Notably, $Dse1^{-/-}$ mice display reduced L-IdoA-blocks and ΔDi2,4S-units and therefore might have an altered growth factor function (Maccarana et al., 2009). Not only the sulfation pattern but also the L-IdoA clusters were altered in the $Dcn^{-/-}$ CS/SD, which could be due to the increased amount of DiS0 and the reduction in 2-O sulfation. The amount of 2-O sulfation in skin CS/DS is only ~2% (Miller et al., 2006). For heparan sulfate/FGF2 interaction there is detailed information describing the importance of L-IdoA and 2-O sulfation in FGF2 binding (Jemth et al., 2002). The 2-O sulfation of the structural homologue DS might be involved in Fgf2 (Penc et al., 1998; Ashikari-Hada et al., 2009) or Fgf7 (Trowbridge and Gallo, 2002) binding and signaling. The amount of GAGs in the wound fluid is 15–65 μg/ml, and DS in wound fluid is a more potent stimulator of Fgf2 signaling than heparan sulfate (Penc et al., 1998). DS from porcine mucosa showed that FGF2 requires sulfated octasaccharides whereas FGF7 requires a sulfated decasaccharide to induce proliferation on FGFR2IIIb transfected BaF3 cells. Even though these studies conclude no impact of 2-O sulfation on BaF3 cell proliferation mediated by FGF7 and -2 (Taylor et al., 2005), the amount of 6.5% ΔDi2,4S in DS from porcine mucosa is even higher than the one determined in the wild-type P30 CS/DS. Interestingly, CS fractions, in contrast to crude extracts, also induced proliferation; however both, CS and DS, required 4-O sulfation (Taylor et al., 2005). $Dcn^{-/-}$ and wild-type highly-sulfated CS/DS preparations showed no differences in the 4-O sulfation; therefore specific 2-O sulfated sequences might be important. It has been shown that addition of exogenous 2-O sulfated heparin oligosaccharides can inhibit Fgf2 binding and signaling, since Fgf is captured by the exogenous polysaccharide. CHO cells deficient in heparan sulfate still exhibit Fgf2 signaling, albeit lower than control cells (Ashikari-Hada et al., 2009) indicating that the remaining CS/DS could support Fgf signaling. This observation confirms our data that FGF7 can bind to wild-type highly-sulfated CS/DS and prevent partially the binding to keratinocytes. In contrast, only at high concentration of $Dcn^{-/-}$ CS/DS binding to keratinocytes is prevented.

To determine the consequences of the reduced amount of 2-O sulfation in $Dcn^{-/-}$ skin CS/DS we analyzed Fgf7 function on keratinocytes (Trowbridge and Gallo, 2002). Although Fgf7 is synthesized by fibroblasts, it only binds to a splice variant of FGFR2 (FGFR2IIIb) expressed by keratinocytes (Werner et al., 2007). We found that primary human keratinocytes display an improved proliferation supported by ERK activation when treated with $Dcn^{-/-}$ highly-sulfated CS/DS alone. This is confirming the positive impact of DS, which is a part of our CS/DS, on keratinocyte proliferation (Trowbridge and Gallo, 2002). The reduced binding of Fgf7 to $Dcn^{-/-}$ undersulfated CS/DS along with altered effects on proliferation and differentiation of keratinocytes might have an impact on epidermal wounds (Taylor et al., 2005) in analogy to the delayed wound healing of EDS patients (Kresse et al., 1987; Shimizu et al., 2011) and $Dcn^{-/-}$ mice (Järveläinen et al., 2006). In the presence of CS/DS, Fgf7 binding to keratinocytes is inhibited by wild-type CS/DS and at higher concentrations also by $Dcn^{-/-}$ CS/DS, indicating that the reduced amount of 2-O sulfation in $Dcn^{-/-}$ CS/DS can also capture Fgf7 (Ashikari-Hada et al., 2009). Cell proliferation is however induced by $Dcn^{-/-}$ CS/DS and one might speculate that this is an example that CS/DS structures are still able to activate the growth factors depending on the organization of the disaccharide units. Notably, addition of DS-decorin to $Dcn^{-/-}$ fibroblast cultures rescues the Fgf7 binding to CS/DS, indicating that DS decorin could be the primary source of binding and modulation of its activity. This is in line to previous published data, where higher concentration of DS promotes Fgf7 binding to the surface of BaF3 cells transfected with the respective receptor FGFR2IIIb. Also, the impact of DS on human primary keratinocytes revealed the same as our data that DS alone induced proliferation was most active with 5 μg/ml in contrast to the 50 μg/ml on BaF3 cells (Trowbridge and Gallo, 2002). In contrast to the previous study, we used complex highly-sulfated CS/DS and did not enzymatically removed CS. Furthermore, our GAG source was from mouse skin including both dermis and epidermis. The impact of both CS/DS preparations on ERK activation was in line with the increased proliferation observed for $Dcn^{-/-}$ CS/DS treatment, but not for wild-type CS/DS treatment.

This shows that structure–activity relationship of GAG-FGF signaling is affected by the loss of DS decorin in skin. Recently, Sterner and co-workers showed that FGF2, which is known to require HS with 2-O sulfation can also use DS with low amount of 2-O sulfation for proliferation indicating that the balance between IdoA and sulfate is important, too (Sterner et al., 2013).

It is well established that 2-D cell cultures do not allow assembly of complex ECM (Florin et al., 2005) and that 3D cultures are more physiologic not only in terms of proper matrix assembly, but also for cell–matrix adhesion (Harunaga and Yamada, 2011). Therefore, we used a 3D co-culture system of fibroblasts embedded in their own ECM (Cukierman et al., 2001; Seidler et al., 2005) upon which we seeded and cultured primary keratinocytes. It is well known that the morphology of keratinocytes depend on the number of fibroblasts (Schoop et al., 1999), and keratinocytes can stimulate fibroblasts to synthesize and secrete growth factors like Fgf7, IL6 and G-CSF (for review: Werner et al., 2007) and induce proliferation and differentiation (Florin et al., 2005). In our co-culture system, primary human keratinocytes grow in multilayer on ECM of fibroblasts and are able to differentiate. To avoid the proliferative effect of the GAGs in the co-cultures, as determined in 2D keratinocyte cultures, we used a lower GAG concentration with similar ERK activation. The suprabasal marker keratin 10 was similarly expressed in both conditions. Surprisingly, the addition of $Dcn^{-/-}$ highly-sulfated GAGs to the 3D co-culture system caused a delayed differentiation compared to the addition of wild-type CS/DS. Overall, primary keratinocytes differentiate faster compared to HaCaT cells (Micallef et al., 2009). Interestingly, the addition of extracted skin CS/DS positively influences the differentiation evoked by wild-type GAGs, supporting the effects of CS/DS seen by others (Trowbridge and Gallo, 2002). The negative effect of $Dcn^{-/-}$ CS/DS on keratinocyte differentiation could be an explanation of the delayed wound healing of $Dcn^{-/-}$ mice (Järveläinen et al., 2006). However, we cannot exclude that in the co-culture of fibroblasts and keratinocytes other factors may play a role. For example, under the co-culture conditions fibroblasts can also synthesize other heparin-binding factors like pleiotrophin or stromal cell derived factor 1 and therefore influence keratinocyte differentiation (Florin et al., 2005). However the changes observed in this study are due to alterations in GAG fine structures caused by lack of DS-decorin that negatively influence keratinocyte differentiation on wild-type 3D fibroblast cultures supporting our hypothesis that DS of decorin is playing an important role in wound healing.

In conclusion, ablation of DS-decorin leads to changes in the composition of CS/DS in skin, specifically causing a decline in 2-O sulfation, thereby altering the bioactivity of these GAGs, pivotal for keratinocyte proliferation and differentiation. The observation that Fgf7 and -2 bioactivity is affected by loss of DS in skin and in $Dcn^{-/-}$ fibroblasts 3D cell culture, together with the fact that Fgf7 binding can be restored by addition of decorin proteoglycan, suggests that DS of decorin is the key molecular factor that triggers Fgf7 signaling and ultimately affects keratinocyte behavior.

4. Experimental procedures

4.1. Decorin-null mice

$Dcn^{-/-}$ mice (Danielson et al., 1997) and wild-type mice were bred in the animal facility in accordance with the German Animal Protection Act (May 25th 1998) and were approved by LANUV, NRW, Germany.

4.2. Materials and methods

The following primary antibodies were used: decorin LF113 (dilution 1:1000; polyclonal rabbit anti-mouse, Fisher et al., 1995), uronyl-2 O sulfotransferase UST D-20 (dilution 1:500, Santa Cruz Biotechnology), collagen type I (dilution 1: 500; polyclonal rabbit; Acris), cytokeratin wide spectrum (dilution 1:250; Abcam), cytokeratin 10 (dilution 1:250; polyclonal rabbit; Abcam), involucrin (dilution 1:250 and 1:400; monoclonal mouse; Thermo Scientific), and pERK1,2 and ERK1,2 (both dilution 1:1000; Cell Signaling). As secondary antibodies Alexa488 rabbit anti-mouse IgG (Molecular Probes, USA) in 1:400 and Alexa647 goat anti-rabbit (Cell Signaling) and for immune blotting anti-rabbit HRP conjugated in 1:1000 were used. Decorin was purified from conditioned medium of human skin fibroblasts as described before (Rühland et al., 2007; Zamfir et al., 2009). The purity of decorin was verified by silver staining after SDS gel electrophoresis.

4.3. 3D cultures of decorin-null and wild-type fibroblasts

Skin fibroblasts were obtained from one-day-old $Dcn^{-/-}$ (Danielson et al., 1997) and wild-type mice. Cells were cultured in modified Eagle's minimum essential medium (MEM) with Earle's salts supplemented with 10% bovine serum (Biochrom, Germany), 2 mM glutamine and 100 U/ml penicillin/0.1 mg/ml streptomycin (PAA, Germany). Cells were used for the following experiments at passage 3 as described previously (Seidler et al., 2005; Rühland et al., 2007). Briefly, 200,000 cells/well were seeded confluent in a 24-well plate or 400,000 cells/12 wells (Falcon, Becton Dickinson, France) and after 24 h the medium was replaced with fresh medium containing 1 mM L-ascorbic acid 2-phosphate (Sigma, Germany) and the 5 μg/ml decorin, or the medium. Cells were cultured for up to 14 days or the indicated time points and medium was changed every second day (Seidler et al., 2005; Rühland et al., 2007). As control for primary wild-type fibroblasts we used 3T3 mouse fibroblasts (ATCC, VA, USA).

4.4. Isolation of epidermal keratinocytes and their cell culture

Primary keratinocytes were isolated from human infantile foreskin (Aasen and Izpisua Belmonte, 2010). Skin was cut into 0.5 cm^2 pieces and decontaminated for 2 h with MEM medium containing 25 mg/l Gentamicin and 25 mg/l Amphotericin. Dispase II treatment (0.5% in PBS, Roche, Germany) of the foreskin over night at 4 °C followed by digestion with trypsin-EDTA for 10 min at 37 °C resulted in isolated keratinocytes. For the following experiments keratinocytes were used in passages 2–3. Also experiments were performed with Celloneer® pooled human juvenile foreskin keratinocytes. The keratinocytes were cultured with Celloneer® medium (PAA).

4.5. Co-cultures of 3D fibroblasts and human primary keratinocytes

Fibroblasts were seeded and cultured for 14 days as described in Section 4.3 to synthesize and deposit their own collagen-rich matrix. ~10^5 primary keratinocytes (53,000 cells/cm^2) were seeded in Celloneer® medium on top of the 3D fibroblast matrices and cultured for 24 h. Co-cultures were treated with 0.1 μg/ml highly-sulfated wild-type and $Dcn^{-/-}$ CS/DS for 72–144 h and monitored every 24 h. Finally, the co-cultures were paraffin embedded and sections analyzed for keratinocyte differentiation.

4.6. Immunofluorescence of 3D co-culture sections

To determine differentiation of keratinocytes the 3D cell cultures were fixed and embedded in paraffin and cut into 4 μm sections. De-waxed sections were fixed and blocked followed by incubation with antibodies against collagen type I (1:500), cytokeratin wide spectrum (1:250), cytokeratin 10 (1:250), and involucrin (1:250) for overnight at 4 °C. Positive cells were detected using the respective secondary fluorescence-conjugated antibody. To rule out unspecific binding of antibodies, negative controls without primary and/or secondary antibodies were performed, respectively. Nuclei were visualized by DAPI. To quantify the fluorescence signals of the keratinocyte markers, control sections were analyzed at different exposure times and gain settings

and converted into grayscale. The final adjustment was an exposure time of 100 ms and a camera gain of 1. The areas of positively-stained keratinocytes were selected and fluorescence signals were quantified in an 8-bit grayscale by surface blot of ImageJ software (rsb.info.nih.gov) (Parsons-Wingerter et al., 2005; Seidler et al., 2006; Jungmann et al., 2012).

4.7. Western blot analysis for decorin, uronyl 2-O sulfotransferase and ERK signaling

Time course experiment (2–10 days) using wild-type fibroblasts cultured in the presence of ascorbate 2-phosphate to generate their own collagen-rich matrix (Stock et al., 2011). 200,000 cells/24-well plate were harvested at days 2, 4, 6, 8 and 10. Protein extracts of cultures were separated under reduced conditions with a 4.5–15% gradient SDS-gel and transfered onto a polyvinylidenedifluoride (PVDF) membrane. Membranes were blocked with 5% skim milk/TBST for 1 h at RT followed by incubation with specific mouse polyclonal antibodies against decorin (a gift from Larry Fisher). 400,000 cells/12-well plate were used to determine Ust. Dermal extracts of *Dcn*$^{-/-}$ and wild-type newborn mice (Jungmann et al., 2012) were also analyzed for Ust expression. Membranes were incubated with anti-rabbit HRP-conjugated secondary antibodies, visualized by enhanced chemiluminescence (Perkin-Elmer Life Sciences, Boston, MA) and monitored with Fusion-SL 4.2 MP (PeqLab, Erlangen, Germany). Blots were stripped with 100 mM β-Mercapto-EtOH, 62.5 mM Tris–HCl and 2% SDS at 50 °C for 30 min and reprobed with β-actin (1:1000) overnight at 4 °C as a loading control.

Human primary keratinocytes (26,000 cells/cm^2) were cultured in 12-well plates as described in Section 4.14. Sub-confluent cells were starved with MCDB 153 medium over night followed by FGF7 or GAG treatment for 30 min. Cells were extracted with a lysis buffer (50 mM Tris/HCl pH 7.5, 150 mM NaCl, 0.5% Triton X-100, 5 mM EDTA) containing cOmplete Mini protease inhibitor and PhosSTOP Mini phosphatase inhibitor (both Roche). 10 μg protein lysates were subjected to SDS-PAGE (12%) followed by immune blotting with the following antibodies: anit-pERK1,2 and reprobed with anti-ERK1,2 and β-actin detected with anti-rabbit HRP-conjugated secondary antibodies as describe for fibroblasts.

The co-cultures of keratinocytes and 3D fibroblasts as described above were treated with RIPA buffer and 4.2 μg of protein extract was used for analysis. For involucrin detection a specific antibody was used in a dilution of 1:400 and as a loading control blots were reprobed with β-actin (1:1000). The signal intensities of involucrin and human β-actin were quantified using ImageJ software.

4.8. Glycosaminoglycan extraction and characterization

GAGs from 3D cell cultures and male mouse skin postnatal stages 30, 45 and 75 mice (P30, 45 and 75) were extracted after the modified protocol (Zamfir et al., 2012). Briefly, 3D cultures and skin samples, from the dorsum of male wild-type and *Dcn*$^{-/-}$ mice, were pre-digested with collagenase B (1 mg/ml) for 24 h at 4 °C, respectively. Proteoglycans were then extracted using guanidinium hydrochloride buffer (4 M guanidinium hydrochloride, 0.05 M sodium acetate, proteinase inhibitors, pH 6.0) by rotation at 4 °C until samples were completely dissolved. Lysates were centrifuged (30 min, 5000 rpm), diluted 1:10 with a starting buffer (0.15 M NaCl, 0.02 M Tris HCl, pH 7.4, 1% Triton X-100) and pre-cleared by DEAE-Ceramic HyperD® F (Pall Life Science, France) anion-exchange-chromatography (Zamfir et al., 2009). CS/DS proteoglycans were eluted with the buffer 1 M NaCl and 0.02 M Tris–HCl, pH = 7.4, dialyzed against the starting buffer and further fractioned by HPLC-DEAE (Seidler et al., 2002) or followed by β-elimination. CS/DS was concentrated using PEG 20000 (Sigma) and dialyzed against ddH_2O.

Glucuronic acid (HexA) concentration was determined in CS/DS extracts with carbazol reaction (Bitter and Muir, 1962). The total sulfate was quantified using the reaction described in Held and Buddecke (1967). Briefly, 100 μl of sample was hydrolyzed with 50 μl of HCl (3 M) for 3 h at 110 °C and cooled to room temperature. Luviskol K90 (2% (w/v)) and $BaCl_2$ (1% (w/v) in H_2O) solution was prepared and added to the sample (100 μl). After rigorous shaking, the reaction was incubated for 30 min RT and measured at OD_{366} using ammonium sulfate as standard (0–4 μM) (Herzog et al., 2011). β-Elimination of the CS/DS was performed overnight at 37 °C using 1:1:1 (v/v/v) solution of the sample, 1 M $NaBH_4$ and 1 M NaOH. The reaction mixture was neutralized with acetic acid (1:10 (v/v)), diluted with the starting buffer and purified with a 0.5 ml DEAE-Ceramic HyperD (Pall) column. Released CS/DS was eluted with 1 M NaCl and desalted. 10 μg CS/DS was depolymerized with 2 × 5 mU chondroitin AC I lyase (Seikagaku Kogyo, Tokyo, Japan) in 200 μl 0.05 M Tris/HCl (pH 8.0), containing 0.06 M sodium acetate, 0.06 M NaCl, 0.01% BSA and 0.003 M NaN_3 for 2 h at 37 °C (Seidler et al., 2002). Oligosaccharides were fractionated on a Superdex Peptide HR10/30 column (Pharmacia, Freiburg, Germany) with 0.5 M NH_4HCO_3 at a flow rate of 0.5 ml/min (Zamfir et al., 2003). Disaccharide CS/DS peaks were pooled and subjected to MS analysis or AMAC derivatization.

4.9. Preparation of CS/DS disaccharides and derivatization with 2-aminoacridone

Ten micrograms of CS/DS was digested with 10 mU chondroitin ABC lyase (Seikagaku, Japan) as described previously (Seidler et al., 2002; Zamfir et al., 2003). Derivatization of the unsaturated disaccharides with 2-aminoacridone (AMAC) was performed by adding 5 μl of 0.1 M AMAC in 15%/85% CH_3COOH/DMSO solution. After incubation for 10 min at RT, 5 μl of $NaBH_3CN$ (1 M) was added and incubated for 16 h at 37 °C. After filling up to 20 μl with DMSO/Glycerol/H_2O solution (2:1:7 (v/v)) (Seidler et al., 2002; Herzog et al., 2011) the AMAC derivatized disaccharides were separated on a 30% borat PAGE and visualized with UV-Transilluminator. As standard for disaccharides we used the unsaturated chondro-disaccharide kit (Seikagaku Corp., Japan) containing Di0S, Di4S, Di6S, Di4,6S and Di2,6S. Furthermore, we used 10 μg CS6S (Sigma) treated as described above as a second standard. Photos were documented with the photo system (Biometra) and band intensities were quantified by ImageJ software.

4.10. mRNA extraction and quantitative real-time PCR

For gene expression analysis fibroblasts were seeded in 24-well plates for indicated period of time (Greiner, Germany). Total RNA was extracted from fibroblasts at different time points using RNeasy Mini Kit and cDNA was synthesized from 2 μg of total RNA using Omiscript RT Kit (all: Qiagen, Germany). mRNA levels of target genes were quantified by real-time RT-PCR using an ABI PRISM 7300 Sequence Detector (Applied Biosystems) and MESA GREEN (Eurogentec, Germany). Amplification was performed in triplicate in a total volume of 25 μl. Raw data were normalized on geometric average of control genes (Vandesompele et al., 2002). The following primer sequences were used: ubiquitin c-F: 5′-GCC CAG TGT TAC CAC CAA G-3′; ubiquitin c-R: 5′-CAC CAA AGA ACA AGC ACA AG-3′; biglycan-F: 5′-CCT GAG ACC CTG AAC GAA C-3′; biglycan-R: 5′-GTG ACC TAA GCC CAA CCT GT-3′; decorin-F: 5′-TGAG CTTCAACAGCATCACC-3′; and decorin-R: 5′-AAGTCATTTTGCCCAACT GC-3′. F—forward primer and R—reverse primer.

4.11. Cloning of SEAP-Fgf7 and SEAP-Fgf8

cDNA encoding murine *Fgf*7 (full length cDNA clone IRAKp961/20112Q) and murine *Fgf*8 (full length cDNA clone) were purchased from imaGenes. To generate a fusion protein with soluble alkaline phosphatase at the N-terminus PCR fragments were generated with specific

primers for Fgf7 or Fgf8, introducing *Xba*I and *Eco*RV restriction sites. The PCR fragments were digested with *Xba*I and *Eco*RV and cloned into the vector gWIZ™ SEAP (Gene Therapy Systems) digested with *Hpa*I and *Xba*I. The plasmids were transformed into DH5α and selected with kanamycin.

4.12. Expression of SEAP fibroblast growth factor fusion proteins and binding assays

HEK293 cells were transfected with Polyfect (Qiagen) and 1.5 μg cDNA for SEAP-Fgf-7, SEAP-Fgf-1 and SEAP-Fgf-8 in MEM containing 10% FBS according to the manufacturer's instructions. 16 h after transfection the medium was changed to serum-free MEM and incubated for 24 h. Successful expression was monitored by alkaline phosphatase assay. AP-Fgf7 expression was confirmed by immune blotting after purification via heparin-sepharose (data not shown). The conditioned medium of HEK293 cells containing the fusion proteins SEAP-Fgf7, SEAP-Fgf1 and SEAP-Fgf8 (Herzog et al., 2011) was used to test whether they bind to the CS/DS proteoglycans extracted from different stages of male mice skin (P30, P45, P60 and P75) and 3D fibroblast cultures. As control 1% bovine serum albumin was used. Briefly, 50 ng proteoglycans were coated to Nunc MaxiSorp plates (Fisher Scientific, Germany) over night at 4 °C in a coating buffer (50 mM NaCl, 100 mM Tris/HCl, pH 7.4). Plates were washed three times with Tris-buffered saline (TBS) and then blocked with 1% BSA/TBS for 1 h at room temperature. SEAP-Fgfs containing conditioned medium (SEAP OD_{405} ~ 1.0) was applied and incubated for 2 h at 37 °C in a binding buffer (150 mM NaCl, 20 mM Tris/HCl, pH7.4). To analyze the binding strength of Fgf7 to the GAGs, wells were incubated for 5 min with a buffer containing 20 mM Tris/HCl and increasing concentration of NaCl (150 mM, 200 mM, 300 mM, 400 mM, 500 mM, 600 mM, 800 mM and 1 M). After washing with TBS, substrate p-nitrophenylphosphate (Sigma, Germany) in diethanolamine (2 mg/ml, pH 9.8) was added. The absorbance was measured at 405 nm, 30 min after incubation at 37 °C using ELISA reader Synergy HT (Biothek).

The cell surface binding assays were performed with confluent primary keratinocytes incubated with conditioned medium containing AP-Fgf7. The medium was supplemented with different concentrations of wild-type and $Dcn^{-/-}$ highly-sulfated CS/DS. Following 2 h incubation cells were washed three times with PBS and the substrate solution was added. The absorbance was measured like described above.

4.13. Digoxigenin labeled FGF2 fibroblast growth factor protein and solid-phase binding assays

Digoxigenin-conjugated FGF2 was prepared as described previously (Ashikari et al., 1995). Briefly, 10 μg of FGF2 (Sigma-Aldrich, Germany) in 0.2 M phosphate buffer, pH 8.5, was added into N-acetylated heparan sulfate and then mixed with 8.75 nmol of digoxigenin-3-O-methylcarbonyl-ε-aminocaproic acid-N hydroxysuccinimide ester (Roche, Germany) in ethanol, followed by incubation for 2 h at room temperature. The Dig-FGF2 solution was purified with a 0.5 ml of heparin-sepharose gel equilibrated with PBST containing 1 mg/ml BSA. Heparin-sepharose gel was washed with 5 ml of PBST containing 1 mg/ml BSA. Dig-FGF2 was eluted with 2 ml of 2 M NaCl in PBST containing 1 mg/ml BSA and dialyzed overnight against PBS. Binding assay was performed as described for AP-Fgfs by incubation of the Dig-FGF2 (~10 ng) with the immobilized CS/DS for 2 h at 37 °C. After washing with PBS, wells were blocked with 1 mg/ml BSA/PBS for 1 h at 4 °C. The wells were washed and alkaline phosphatase-conjugated Fab fragments of the anti-digoxigenin antibody (1:1000) were added for 1 h at room temperature. Unbound Fab fragments were washed with PBS/Tween 20 0.05% (v/v), and the alkaline phosphatase substrate was added for 30 min at 37 °C as described above. Statistical analyses were performed with GraphPad Prism 4, using Mann–Whitney test. Values of $P < 0.05$ were taken as significant.

4.14. Proliferation and metabolic activity of human primary keratinocytes

Primary human keratinocytes were seeded in 96-well plates and cultured as described above until 50–60% confluence. The medium was replaced by MCDB 153 (Biochrom, Germany) complete medium containing 0.001 to 5 μg/ml CS/DS GAGs. MCDB 153 complete medium was used as control, whereas Celloneer® medium was the positive control. BrdU labeling solution was added after 24 h for 16 h. BrdU cell proliferation ELISA was carried out according to the manufacturer's instructions (Roche) and measured at 450 nm with the ELISA reader Synergy HT. Results are expressed as means ± SD of one representative experiment performed in triplicate. Three independent experiments in triplicate were performed. FGF7 stimulation was carried out with 5 ng/ml FGF7 (Sigma) in MCDB153 medium as descried previously (Trowbridge and Gallo, 2002). 5–6 independent experiments were carried out in triplicate. Data were compared by non-parametric analysis (GraphPad Prism software) using the Mann–Whitney test for independent groups. Metabolic activity was monitored by the MTT assay. Keratinocytes were seeded and treated with different GAGs as described above following incubation with MTT solution over night. The supernatant was removed and the crystals dissolved in DMSO followed by photometric measurements at 490 nm with the ELISA reader Synergy HT.

Supplementary data to this article can be found online at http://dx.doi.org/10.1016/j.matbio.2014.01.003.

Author's contribution

KN extracted, characterized the GAGs from mice dermis and established the Fgf binding assays, JKR extracted keratinocytes and performed all keratinocyte and co-culture experiments, OJ extracted the GAGs, KG cloned the AP-Fgf1 and 8 and drafted the manuscript, RVI provided the $Dcn^{-/-}$ mice and drafted the manuscript, ADZ performed the MS/MS analysis, and DGS designed the study, interpreted the data and drafted the manuscript.

Acknowledgments

We thank Margret Bahl for her expert technical assistance and Dr. Larry Fisher for the generous gift of decorin antiserum. We thank Prof. Dr. Lydia Sorokin for the opportunity to access the confocal microscope.

References

Aasen, T., Izpisua Belmonte, J.C., 2010. Isolation and cultivation of human keratinocytes from skin or plucked hair for the generation of induced pluripotent stem cells. Nat. Protoc. 5, 371–382.

Ashikari, S., Habuchi, H., Kimata, K., 1995. Characterization of heparan sulfate oligosaccharides that bind to hepatocyte growth factor. J. Biol. Chem. 270, 29586–29593.

Ashikari-Hada, S., Habuchi, H., Sugaya, N., Kobayashi, T., Kimata, K., 2009. Specific inhibition of FGF-2 signaling with 2-O-sulfated octasaccharides of heparin sulfate. Glycobiology 19, 644–654.

Bartolini, B., Thelin, M.A., Svensson, L., Ghiselli, G., van Kuppevelt, T.H., Malmström, A., Maccarana, M., 2013. Iduronic acid in chondroitin/dermatan sulfate affects directional migration of aortic smooth muscle cells. PLoS One 8, e66704.

Bitter, T., Muir, H.M., 1962. A modified uronic acid carbazole reaction. Anal. Biochem. 4, 330–334.

Bocian, C., Urbanowitz, A.-K., Owens, R.T., Iozzo, R.V., Götte, M., Seidler, D.G., 2013. Decorin potentiates IFN-γ activity in a model of allergic inflammation. J. Biol. Chem. 288, 12699–12711.

Brandan, E., Gutierrez, J., 2013. The role of skeletal muscle proteoglycans during myogenesis. Matrix Biol. 32, 289–297.

Cheng, F., Heinegard, D., Malmström, A., Schmidtchen, A., Yoshida, K., Fransson, L.-A., 1994. Patterns of uronosyl epimerization and 4-/6-O-sulphation in chondroitin/dermatan sulphate from decorin and biglycan of various bovine tissues. Glyobiology 4, 655–696.

Cukierman, E., Pankov, R., Stevens, D.R., Yamada, K.M., 2001. Taking cell–matrix adhesions to the third dimension. Science 294, 1708–1712.

Danielson, K.G., Baribault, H., Holmes, D.F., Graham, H., Kadler, K.E., Iozzo, R.V., 1997. Targeted disruption of decorin leads to abnormal collagen fibril morphology and skin fragility. J. Cell Biol. 136, 729–743.

Dunkmann, A.A., Buckley, M.R., Mienaltowski, M.J., Adams, S.M., Thomas, S.J., Satchell, L., Kumar, A., Pathmanathan, L., Beason, D.P., Iozzo, R.V., Birk, D.E., Soslovski, L.J., 2013. Decorin expression is important in tendon structure and mechanical properties. Matrix Biol. 32, 3–13.

Faiyaz-Ul-Haque, M., Zaidi, S.H., Al Ali, M., Al Mureikhi, M.S., Kennedy, S., Al Thani, G., Tsui, L.C., Teebi, A., 2004. A novel missense mutation in the galactosyltransferase-I (B4GALT7) gene in a family exhibiting facioskeletal anomalies and Ehlers–Danlos syndrome resembling the progeroid type. Am. J. Med. Genet. 128A, 39–45.

Ferdous, Z., Peterson, S.B., Tseng, H., Anderson, D.K., Iozzo, R.V., Grande-Allen, K.J., 2010. A role for decorin in controlling proliferation, adhesion, and migration of murine embryonic fibroblasts. J. Biomed. Mater. Res. A 93, 419–428.

Fernandez-Botran, R., Yan, J., Justus, D.E., 1999. Binding of interferon gamma by glycosaminoglycans: a strategy for localization and/or inhibition of its activity. Cytokine 11, 313–325.

Fisher, L.W., Stubbs III, J.T., Young, M.F., 1995. Antisera and cDNA probes to human and certain animal model bone matrix noncollagenous proteins. Acta Orthop. Scand. Suppl. 266, 61–65.

Florin, L., Maas-Szabowski, N., Werner, S., Szabowski, A., Angel, P., 2005. Increased keratinocyte proliferation by JUN-dependent expression of PTN and SDF-1 in fibroblasts. J. Cell Sci. 118, 1981–1989.

Harunaga, J.S., Yamada, K.M., 2011. Cell–matrix adhesions in 3D. Matrix Biol. 30, 363–368.

Held, E., Buddecke, E., 1967. Studies on the chemistry of the arterial wall, XI. Demonstration, purification and properties of a chondroitin-4-sulfatase from bovine aorta. Hoppe Seylers Z. Physiol. Chem. 348, 1047–1060.

Herzog, C., Lippmann, I., Grobe, K., Zamfir, A.D., Echtermeyer, F., Seidler, D.G., 2011. The amino acid tryptophan prevents the biosynthesis of dermatan sulfate. Mol. Biosyst. 7, 2872–2881.

Inoue, Y., Inouye, Y., Nagasawa, K., 1990. Conformational equilibria of the L-iduronate residue in non-sulphated di-, tetra- and hexa-saccharides and their alditols derived from dermatan sulphate. Biochem. J. 265, 533–538.

Iozzo, R.V., 1997. The family of the small leucine-rich proteoglycans: key regulators of matrix assembly and cellular growth. Crit. Rev. Biochem. Mol. Biol. 32, 141–174.

Iozzo, R.V., Murdoch, A., 1996. Proteoglycans of the extracellular environment: clues from the gene and protein side offer novel perspectives in molecular diversity and function. FASEB J. 10, 598–614.

Järveläinen, H., Puolakkainen, P., Pakkanen, S., Brown, E.L., Hook, M., Iozzo, R.V., Sage, E.H., Wight, T.N., 2006. A role for decorin in cutaneous wound healing and angiogenesis. Wound Repair Regen. 14, 443–452.

Jemth, P., Kreuger, J., Kusche-Gullberg, M., Sturiale, L., Gimenez-Gallego, G., Lindahl, U., 2002. Biosynthetic oligosaccharide libraries for identification of protein-binding heparan sulfate motifs. Exploring the structural diversity by screening for fibroblast growth factor (FGF)1 and FGF2 binding. J. Biol. Chem. 277, 30567–30573.

Jung, J.W., Cha, S.H., Lee, S.C., Chun, I.K., Kim, Y.P., 1997. Age-related changes of water content in the rat skin. J. Dermatol. Sci. 14, 12–19.

Jungmann, O., Nikolovska, K., Stock, C., Schulz, J.N., Eckes, B., Riethmüller, C., Owens, R.T., Iozzo, R.V., Seidler, D.G., 2012. The dermatan sulfate proteoglycan decorin modulates α2β1 integrin and the vimentin intermediate filament system during collagen synthesis. PLoS One 7, e50809.

Kobayashi, M., Sugumaran, G., Liu, J., Shworak, N.W., Silbert, J.E., Rosenberg, R.D., 1999. Molecular cloning and characterization of a human uronyl 2-sulfotransferase that sulfates iduronyl and glucuronyl residues in dermatan/chondroitin sulfate. J. Biol. Chem. 274, 10474–10480.

Kresse, H., Rosthoj, S., Quentin, E., Hollmann, J., Glössl, J., Okada, S., Tønnesen, T., 1987. Glycosaminoglycan-free small proteoglycan core protein is secreted by fibroblasts from a patient with a syndrome resembling progeroid. Am. J. Hum. Genet. 41, 436–453.

Maccarana, M., Kalamajski, S., Kongsgaard, M., Magnusson, S.P., Oldberg, A., Malmström, A., 2009. Dermatan sulfate epimerase 1-deficient mice have reduced content and changed distribution of iduronic acids in dermatan sulfate and an altered collagen structure in skin. Mol. Cell. Biol. 29, 5517–5528.

Malmström, A., Bartolini, B., Thelin, M.A., Pacheco, B., Maccarana, M., 2012. Iduronic acid in chondroitin/dermatan sulfate: biosynthesis and biological function. J. Histochem. Cytochem. 60, 916–925.

Micallef, L., Belaubre, F., Pinon, A., Jayat-Vignoles, C., Delage, C., Charveron, M., Simon, A., 2009. Effects of extracellular calcium on the growth-differentiation switch in immortalized keratinocyte HaCaT cells compared with normal human keratinocytes. Exp. Dermatol. 18, 143–151.

Miller, M.J., Costello, C.E., Malmström, A., Zaia, J., 2006. A tandem mass spectrometric approach to determination of chondroitin/dermatan sulfate oligosaccharide glycoforms. Glycobiology 16, 502–513.

Miyake, N., Kosho, T., Mizumoto, S., Furuichi, T., Hatamochi, A., Nagashima, Y., Arai, E., Takahashi, K., Kawamura, R., Wakui, K., Takahashi, J., Kato, H., Yasui, H., Ishida, T., Ohashi, H., Nishimura, G., Shiina, M., Saitsu, H., Tsurusaki, Y., Doi, H., Fukushima, Y., Ikegawa, S., Yamada, S., Sugahara, K., Matsumoto, N., 2010. Loss-of-function mutations of CHST14 in a new type of Ehlers–Danlos syndrome. Hum. Mutat. 31, 966–974.

Mulloy, B., Forster, M.J., 2000. Conformation and dynamics of heparin and heparan sulfate. Glycobiology 10, 1147–1156.

Parsons-Wingerter, P., Kasman, I.M., Norberg, S., Magnussen, A., Zanivan, S., Rissone, A., Baluk, P., Favre, C.J., Jeffry, U., Murray, R., McDonald, D.M., 2005. Uniform overexpression and rapid accessibility of alpha5beta1 integrin on blood vessels in tumors. Am. J. Pathol. 167, 193–211.

Penc, S.F., Pomahac, B., Winkler, T., Dorschner, R.A., Eriksson, E., Herndon, M., Gallo, R.L., 1998. Dermatan sulfate released after injury is a potent promoter of fibroblast growth factor-2 function. J. Biol. Chem. 273, 28116–28121.

Rühland, C., Schönherr, E., Robenek, H., Hansen, U., Iozzo, R.V., Bruckner, P., Seidler, D.G., 2007. The glycosaminoglycan chain of decorin plays an important role in collagen fibril formation at the early stages of fibrillogenesis. FEBS J. 274, 4246–4255.

Sarrazin, S., Lamanna, W.C., Esko, J.D., 2011. Heparan sulfate proteoglycans. Cold Spring Harb. Perspect. Biol. 3 (pii: a004952).

Schaefer, L., Iozzo, R.V., 2008. Biological functions of the small leucine-rich proteoglycans: from genetics to signal transduction. J. Biol. Chem. 283, 2135–2139.

Schaefer, L., Iozzo, R.V., 2012. Small leucine-rich proteoglycans, at the crossroad of cancer growth and inflammation. Curr. Opin. Genet. Dev. 22, 56–57.

Scholzen, T., Solursh, M., Suzuki, S., Reiter, R., Morgan, J.L., Buchberg, A.M., Siracusa, L.D., Iozzo, R.V., 1994. The murine decorin: complete cDNA cloning, genomic organization, chromosomal assignment and expression during organogenesis and tissue differentiation. J. Biol. Chem. 269, 28270–28281.

Schoop, V.M., Mirancea, N., Fusenig, N.E., 1999. Epidermal organization and differentiation of HaCaT keratinocytes in organotypic co-cultures with human dermal fibroblasts. J. Invest. Dermatol. 112, 343–353.

Seidler, D.G., 2012. The galactosaminoglycan-containing decorin and its impact on diseases. Curr. Opin. Struct. Biol. 22, 578–582.

Seidler, D.G., Dreier, R., 2008. Decorin and its galactosaminoglycan chain: extracellular regulator of cellular function? IUBMB Life 60, 729–733.

Seidler, D.G., Breuer, E., Grande-Allen, K.J., Hascall, V.C., Kresse, H., 2002. Core protein dependence of epimerization of glucuronosyl residues in galactosaminoglycans. J. Biol. Chem. 277, 42409–42416.

Seidler, D.G., Schaefer, L., Robenek, H., Iozzo, R.V., Kresse, H., Schönherr, E., 2005. A physiologic three-dimensional cell culture system to investigate the role of decorin in matrix organisation and cell survival. Biochem. Biophys. Res. Commun. 332, 1162–1170.

Seidler, D.G., Faiyaz-Ul-Haque, M., Hansen, U., Yip, G.W., Zaidi, S.H., Teebi, A.S., Kiesel, L., Götte, M., 2006. Defective glycosylation of decorin and biglycan, altered collagen structure, and abnormal phenotype of the skin fibroblasts of an Ehlers–Danlos syndrome patient carrying the novel Arg270Cys substitution in galactosyltransferase I (beta4GalT-7). J. Mol. Med. 84, 583–594.

Seidler, D.G., Mohamed, N.A., Bocian, C., Stadtmann, A., Hermann, S., Schafers, K., Schafers, M., Iozzo, R.V., Zarbock, A., Götte, M., 2011. The role for decorin in delayed-type hypersensitivity. J. Immunol. 187, 6108–6119.

Shimizu, K., Okamoto, N., Miyake, N., Taira, K., Sato, Y., Matsuda, K., Akimaru, N., Ohashi, H., Wakui, K., Fukushima, Y., Matsumoto, N., Kosho, T., 2011. Delineation of dermatan 4-O-sulfotransferase 1 deficient Ehlers–Danlos syndrome: observation of two additional patients and comprehensive review of 20 reported patients. Am. J. Med. Genet. A 155A, 1949–1958.

Sterner, E., Meli, L., Kwon, S.J., Dordick, J.S., Linhardt, R.J., 2013. FGF–FGFR signaling mediated through glycosaminoglycans in microtiter plate and cell-based microarray platforms. Biochemistry 52, 9009–9019.

Stock, C., Jungmann, O., Seidler, D.G., 2011. Decorin and chondroitin-6 sulfate inhibit B16V melanoma cell migration and invasion by cellular acidification. J. Cell. Physiol. 226, 2641–2650.

Sugahara, K., Mikami, T., Uyama, T., Mizuguchi, S., Nomura, K., Kitagawa, H., 2003. Recent advances in the structural biology of chondroitin sulfate and dermatan sulfate. Curr. Opin. Struct. Biol. 13, 612–620.

Taylor, K.R., Rudisill, J.A., Gallo, R.L., 2005. Structural and sequence motifs in dermatan sulfate for promoting fibroblast growth factor-2 (FGF-2) and FGF-7 activity. J. Biol. Chem. 280, 5300–5306.

Trowbridge, J.M., Gallo, R.L., 2002. Dermatan sulfate: new functions from an old glycosaminoglycan. Glycobiology 12, 117R–125R.

Vandesompele, J., De Preter, K., Pattyn, F., Poppe, B., Van Roy, N., De Paepe, A., Speleman, F., 2002. Accurate normalization of real-time quantitative RT-PCR data by geometric averaging of multiple internal control genes. Genome Biol. 3 (RESEARCH0034).

Werner, S., Grose, R., 2003. Regulation of wound healing by growth factors and cytokines. Physiol. Rev. 83, 835–870.

Werner, S., Krieg, T., Smola, H., 2007. Keratinocyte–fibroblast interactions in wound healing. J. Invest. Dermatol. 127, 998–1008.

Xu, R., Ori, A., Rudd, T.R., Uniewicz, K.A., Ahmed, Y.A., Guimond, S.E., Skidmore, M.A., Siligardi, G., Yates, E.A., Fernig, D.G., 2012. Diversification of the structural determinants of fibroblast growth factor–heparin interactions; implications for binding specificity. J. Biol. Chem. 287, 40061–40073.

Zamfir, A., Seidler, D.G., Kresse, H., Peter-Katalinic, J., 2003. Structural investigation of chondroitin/dermatan sulfate oligosaccharides from human skin fibroblast decorin. Glycobiology 13, 733–742.

Zamfir, A.D., Flangea, C., Sisu, E., Serb, A.F., Dinca, N., Bruckner, P., Seidler, D.G., 2009. Analysis of novel over- and under-sulfated glycosaminoglycan sequences by enzyme cleavage and multiple stage MS. Proteomics 9, 3435–3444.

Zamfir, A.D., Flangea, C., Serb, A., Sisu, E., Zagrean, L., Rizzi, A., Seidler, D.G., 2012. Brain chondroitin/dermatan sulfate, from cerebral tissue to fine structure: extraction, preparation, and fully automated chip-electrospray mass spectrometric analysis. Methods Mol. Biol. 836, 145–159.

Zhao, X., Yang, B., Solakylidirim, K., Joo, E.J., Toida, T., Higashi, K., Linhardt, R.J., Li, L., 2013. Sequence analysis and domain motifs in the porcine skin decorin glycosaminoglycan chain. J. Biol. Chem. 288, 9226–9237.